International Journal of Nanomedicine

Dovepress
open access to scientific and medical research

Open Access Full Text Article

ORIGINAL RESEARCH

RGD-tagged helical rosette nanotubes aggravate acute lipopolysaccharide-induced lung inflammation

This article was published in the following Dove Press journal:
International Journal of Nanomedicine
5 December 2011
Number of times this article has been viewed

Sarabjeet Singh Suri[1]
Steven Mills[1]
Gurpreet Kaur Aulakh[1]
Felaniaina Rakotondradany[2]
Hicham Fenniri[2]
Baljit Singh[1]

[1]Department of Veterinary Biomedical Sciences, University of Saskatchewan, Saskatoon; [2]National Institute for Nanotechnology and Department of Chemistry, Edmonton, Canada

Abstract: Rosette nanotubes (RNT) are a novel class of self-assembled biocompatible nanotubes that offer a built-in strategy for engineering structure and function through covalent tagging of synthetic self-assembling modules (G∧C motif). In this report, the G∧C motif was tagged with peptide Arg-Gly-Asp-Ser-Lys (RGDSK-G∧C) and amino acid Lys (K-G∧C) which, upon co-assembly, generate RNTs featuring RGDSK and K on their surface in predefined molar ratios. These hybrid RNTs, referred to as K^x/$RGDSK^y$-RNT, where x and y refer to the molar ratios of K-G∧C and RGDSK–G∧C, were designed to target neutrophil integrins. A mouse model was used to investigate the effects of intravenous K^x/$RGDSK^y$-RNT on acute lipopolysaccharide (LPS)-induced lung inflammation. Healthy male C57BL/6 mice were treated intranasally with *Escherichia coli* LPS 80 μg and/or intravenously with K^{90}/$RGDSK^{10}$-RNT. Here we provide the first evidence that intravenous administration of K^{90}/$RGDSK^{10}$-RNT aggravates the proinflammatory effect of LPS in the mouse. LPS and K^{90}/$RGDSK^{10}$-RNT treatment groups showed significantly increased infiltration of polymorphonuclear cells in bronchoalveolar lavage fluid at all time points compared with the saline control. The combined effect of LPS and K^{90}/$RGDSK^{10}$-RNT was more pronounced than LPS alone, as shown by a significant increase in the expression of interleukin-1β, MCP-1, MIP-1, and KC-1 in the bronchoalveolar lavage fluid and myeloperoxidase activity in the lung tissues. We conclude that K^{90}/$RGDSK^{10}$-RNT promotes acute lung inflammation, and when used along with LPS, leads to exaggerated immune response in the lung.

Keywords: RGD peptide, helical rosette nanotubes, neutrophils, macrophages, chemokines, inflammation

Introduction

Nanotechnology is a rapidly growing multidisciplinary field dealing among other things with the creation and investigation of functional materials/devices by manipulating matter in the nanoscale range (approximately 1–100 nm). Because of their unique physical and chemical properties, nanostructured materials and associated technologies are anticipated to have a market of US$1 trillion by 2015.[1,2] Among these materials, carbon and metallic nanotubes are extensively studied for a wide variety of biomedical applications due to their unique mechanical and electronic properties. However, these materials suffer from poor solubility, lack of reproducibility of the medical applications associated with them, and cytotoxicity.[3–5] Therefore, biocompatible protein-based or peptide-based nanotubes, offer an attractive alternative for biomedical applications.[3]

Rosette nanotubes (RNTs) are a novel class of biologically inspired and biocompatible nanomaterials.[6–8] RNTs are obtained by spontaneous self-assembly of a

Correspondence: Baljit Singh
Department of Veterinary Biomedical Sciences, University of Saskatchewan, Saskatoon, SK, S7N5B4, Canada
Tel +1 306 966 7068
Fax +1 306 966 7274
Email baljit.singh@usask.ca

Dr Hicham Fenniri
National Institute for Nanotechnology and Department of Chemistry,
11421 Saskatchewan Drive,
Edmonton, AB T6G2M9, Canada
Email: hicham.fenniri@ualberta.ca

synthetic heterobicyclic G∧C motif featuring the Watson–Crick H-bond donor/acceptor arrays of guanine and cytosine (Figure 1).[7] Hierarchical self-assembly of the G∧C motif proceeds via formation of six-membered supermacrocycles (rosettes) maintained by 18 H bonds, which then stack up to form nanotubes approximately 3.5 nm in diameter with an inner channel of 1.1 nm.[6–11] The outer diameter varies depending on substitutions on the G∧C motif expressed on the outer surface of the resulting nanotubes. The length of the tube is regulated through a variety of factors, including temperature and concentration.[12] Upon self-assembly, in principle any functional group covalently attached to the G∧C motif could be expressed on the surface of the nanotubes, thereby offering a robust built-in strategy for manipulating the physical and biological properties of RNTs for specific medical or biological applications.

We have recently shown that intratracheal administration of lysine-functionalized RNT (assembled from twin G∧C bases) in C57BL/6 mice induces mild and transient inflammation in the lung.[13] Our in vitro study showed that K-RNT (assembled form K-G∧C) neither reduces cell viability nor induces robust inflammation in human bronchial epithelial adenocarcinoma Calu-3 cells and macrophages.[12,14] We also co-assembled K-G∧C with a G∧C module bearing Arg-Gly-Asp-Ser-Lys (RGDSK) peptide in a 90:10 molar ratio, resulting in hybrid RNT (K^{90}/$RGDSK^{10}$-RNT), specifically to target integrins, a family of heterodimeric transmembrane proteins that recognize the RGD peptide sequence.[15] We have also demonstrated that K^{90}/$RGDSK^{10}$-RNT induces activation of P38 mitogen-activated protein kinase and overexpression of proapoptotic genes, leading to DNA fragmentation in human adenocarcinoma cells.[16] These results suggest that K^{90}/$RGDSK^{10}$-RNT could be used as a drug to induce apoptosis or as a versatile platform to deliver a variety of biologically active molecules.

Acute inflammation accompanies many respiratory diseases and is characterized by recruitment of activated neutrophils into the lungs.[17] Activated neutrophils, although critical for the host defense, are also credited with causing excessive tissue damage, morbidity, and mortality.[18] Neutrophils are recruited through a complex interplay of chemokines and adhesive proteins, such as integrins and selectins expressed on the vascular endothelium and blood cells.[19] The role of integrins in causing firm adhesion of neutrophils to the endothelium and activation

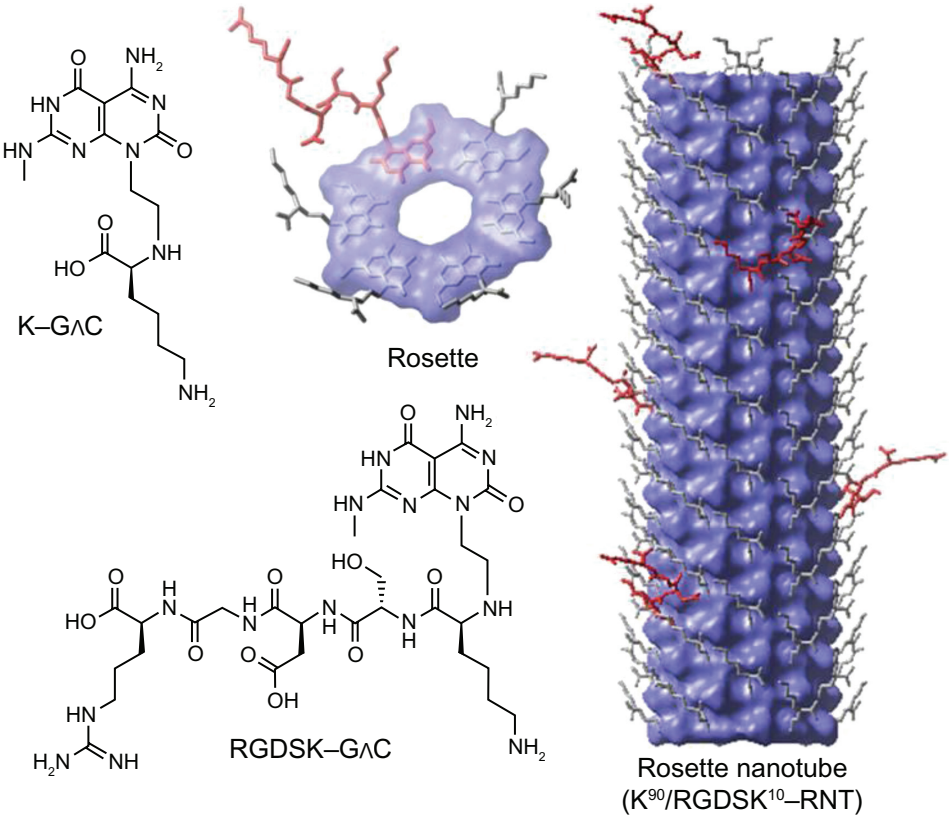

Figure 1 Hierarchical self-assembly of rosette nanotubes. The G∧C motif functionalized with K and RGDSK self-assemble into six-membered supermacrocycles (rosettes), which then stack up to form rosette nanotubes. K–G∧C and RGDSK–G∧C can be co-assembled in a predefined molar ratio to form hybrid rosette nanotubes, such as the K^{90}/$RGDSK^{10}$-RNT investigated in this report.

of signaling is well established.[20] Because of the ability of K^{90}/RGDSK[10]-RNT to target integrin $\alpha_v\beta_3$ expressed on neutrophils and the endothelium,[21,22] we studied the effects of this hybrid RNT on the very early stages, including neutrophil migration and cytokine expression of acute lung inflammation in a mouse model.

Materials and methods

RNT synthesis

K and RGDSK-functionalized GC bases were prepared as previously reported.[8,23,24] A stock solution of RNTs (1 mg/mL) was prepared by co-assembling K-G∧C and RGDSK-G∧C in a 10:90 molar ratio and diluted to the desired concentration as indicated in the following experiments.

Animals

Six to eight week-old healthy male C57BL/6 mice procured from the Animals Resource Centre at the University of Saskatchewan, Canada, were used for this study. All animal protocols used in this study were approved by the University of Saskatchewan Committee on Animal Care Assurance in accordance with the Canadian Council on Animal Care guidelines. The animals were acclimatized for a period of one week in the animal care unit prior to experimentation, and had access to food and water ad libitum. The mice (22–28 g) were randomly assigned to treatment groups. All personnel involved in the analyses were blinded to the treatment groups.

Treatments

Mice were treated intranasally with 80 µg *Escherichia coli* 0127.B8 lipopolysaccharide (LPS, Sigma-Aldrich, Oakville, ON, Canada) and/or K^{90}/RGDSK[10]-RNT (12.5 µL intravenously) at the same time. Untreated control mice were given an equal volume of saline. Approximately 3, 6, or 12 hours following exposure, mice were euthanized by cervical dislocation under light anesthesia (5 mg/mL ketamine-xylazine per 100 g body weight, intraperitoneally).

Sample collection, processing and cell counts

Blood, bronchoalveolar lavage fluid, and lung samples were collected. Blood was collected by cardiac puncture and processed for evaluation of total leukocyte counts on the hemocytometer. Bronchoalveolar lavage was performed by washing the whole lung with ice-cold Hanks Balanced Salt Solution (3 × 1 mL, Sigma-Aldrich) as described elsewhere.[25] A total cell count was performed using a standard hemocytometer.

One lung was fixed in freshly prepared paraformaldehyde 4% in phosphate-buffered solution (pH 7.4) for 16 hours. Pieces of the lobes were later processed through ascending grades of alcohol and then embedded in paraffin. Tissue blocks were cut into 5 µm sections for light microscopy. Hematoxylin and eosin-stained sections were used for histopathological evaluation. For protein and mRNA analysis, lung tissues were snap-frozen in liquid nitrogen and stored at −80°C until analysis.

Histopathology

Sections prepared from paraffin-embedded blocks and stained with hematoxylin and eosin were evaluated by two independent observers. The tissue changes were subjectively graded for no inflammation, mild inflammation, and high inflammation.

Myeloperoxidase assay

Lung tissues were homogenized in 50 mM HEPES (pH 8.0) containing 0.5% CTAC and cell-free extract, and stored at −20°C until further use. Samples were diluted in phosphate citrate buffer (pH 5.0). A myeloperoxidase assay was performed on lung tissues from each treatment group as described elsewhere.[26] Absorbance was read using a NOVOstar microplate reader (BMG Labtech, Durham, NC) set at 450 nm, and the change in OD/min was calculated.

Total protein in bronchoalveolar lavage samples

Bronchoalveolar lavage protein concentration was used as an indicator of blood-pulmonary epithelial barrier integrity. Total protein was measured by using the Bradford dye binding assay (Bio-Rad Laboratories, Hercules, CA) with bovine serum albumin as a standard.

Enzyme-linked immunosorbent assay

An enzyme-linked immunosorbent assay was conducted on the lung tissue. Frozen lung samples were homogenized in lysis buffer (150 mM sodium chloride, 1% NP-40, 0.5% sodium deoxycholate, 0.1% sodium dodecyl sulfate, 50 mM Tris pH 8.0, 5 mM EDTA, protease inhibitor cocktail 100 µL/10 mL). Homogenates were collected after centrifuging the samples at 25,000 g for 15 minutes at 4°C. For quantification, duplicate samples from four mice were used for each treatment. Interleukin-1β, MCP-1, MIP-2, and KC-1 were quantified by sandwich enzyme-linked immunosorbent assay kits (R&D Systems, Minneapolis, MN) as per the manufacturer's instructions. Recombinant standards were purchased from

R&D Systems. Absorbance was read using the NOVOstar microplate reader set at 450 nm.

Real time reverse-transcriptase polymerase chain reaction

RNA was isolated from lung samples and purified using the RNase mini kit followed by RNase-free DNase treatment (Qiagen, Mississauga, ON, Canada). RNA integrity was confirmed by agarose gel electrophoresis and quantified with Nanodrop spectrophotometry (Thermo Fisher Scientific, Ottawa, ON). The mRNA was reverse transcribed using the QuantiTect reverse transcription kit (Qiagen) with a mixture of universal oligo dT and random primers as per the manufacturer's instructions. The cDNA generated by this method was used for reverse-transcriptase polymerase chain reaction analysis of the expression of interleukin-1β (GenBank Accession No BC011437), MCP-1 (GenBank Accession No NM_011333), MIP-1 (GenBank Accession No NM_011337), and KC-1 (GenBank Accession No NM_008176) using QuantiFast SYBR Green polymerase chain reaction kit (Qiagen, Canada). The glyceraldehyde-3-phosphate dehydrogenase gene (GAPDH, GenBank Accession No. BC096042) was used as the reference housekeeping gene. The reactions were performed using the primer pairs; 5′-ATGGCAACTGTTCCTGAACTC-3′ and 5′-CTGCCTGAAGCTCTTGTTGAT-3′ for interleukin-1β, 5′-ATGAAGGTCTCCACCACTG-3′ and 5′-GCAAAGGCTGCTGGTTTCA-3′ for MIP-1, 5′-ATGCAGGTCCCTGTCATGC-3′ and 5′-GCTGCTGGTGATCCTCTTGTA-3′ for MCP-1, 5′-AGTGCCTGCAGACCATGG-3′ and 5′-CTTGCCTTGACCCTGAAGC-3′ for KC-1, and 5′-TGCATCCTGCACCACCAACTG-3′ and 5′-GGGCCATCCACAGTCTTCTGG-3′ for GAPDH. The negative control consisted of all the components of the reaction mixture except RNA. Real-time polymerase chain reaction analysis was performed using the MX3005P Light-Cycler (Stratagene, La Jolla, CA) as per the manufacturer's instructions. The cDNA was denatured for 5 minutes at 95°C, followed by amplification of target DNA through 45 cycles of denaturation at 95°C for 30 seconds, annealing at 55°C for 30 seconds, and extension at 60°C for 45 seconds. Relative expression levels were calculated after correction for expression of GAPDH using MxPro software.

Statistical analysis

Data are the average of n = 4 for the experimental groups and n = 6 for controls. Values are expressed as the mean ± standard deviation. Statistical analysis was carried out with SigmaStat 3.0 statistical software (Systat Inc, Chicago, IL). Values represent the means ± standard deviation. Comparisons between groups were performed using one-way analysis of variance. Differences were considered significant at $P < 0.05$.

Results

Lung histology

We used a mouse model to investigate the effects of intravenous K^{90}/$RGDSK^{10}$-RNT on LPS-induced acute lung inflammation. Hematoxylin and eosin staining of lung sections showed normal lung morphology in saline control mice (Figure 2A and B). Intravenous treatment with K^{90}/$RGDSK^{10}$-RNT (Figure 2C and D), intranasal administration

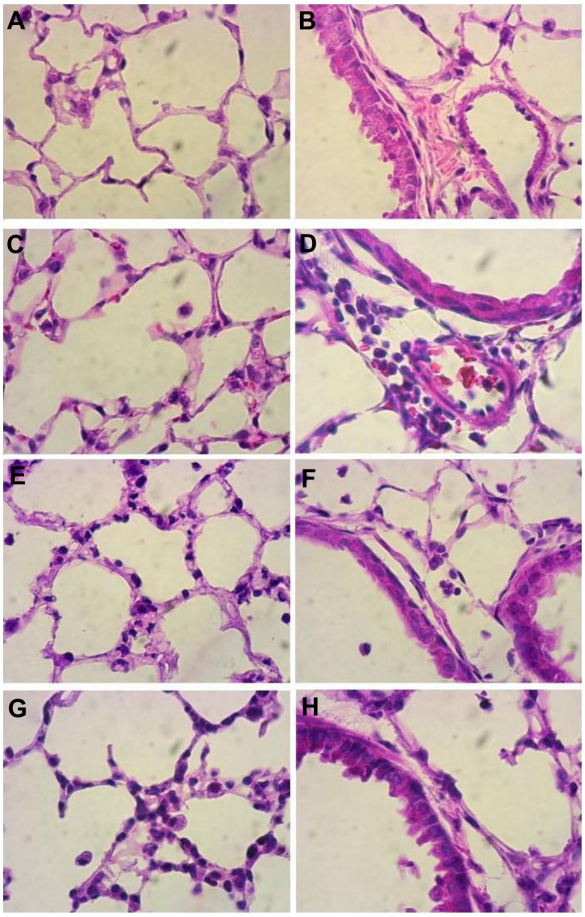

Figure 2 Histopathology of lung sections. Lungs from mice treated intranasally with 80 μg lipopolysaccharide and/or K^{90}/$RGDSK^{10}$ rosette nanotubes (5%, 12.5 μL intravenously) and saline controls were evaluated using sections stained with hematoxylin and eosin. Control lung tissue showed no inflammation and normal lung architecture (**A**, **B**), whereas mice treated with K^{90}/$RGDSK^{10}$ rosette nanotubes (**C**, **D**), lipopolysaccharide (**E**, **F**), and lipopolysaccharide + K^{90}/$RGDSK^{10}$ rosette nanotubes (**G**, **H**) showed septal neutrophilic infiltration, leukocytes adhering to the blood vessel wall, perivascular infiltration of leukocytes, and peribronchiolar accumulation of neutrophils at the 12-hour time point.

of *E. coli* LPS (Figure 2E and F), or both (Figure 2G and H), caused some signs of inflammation, such as septal congestion and accumulation of inflammatory cells.

Differential cell count in bronchoalveolar lavage fluid

Total and differential cell counts were performed in bronchoalveolar lavage fluid. Mice treated with LPS and/or K^{90}/$RGDSK^{10}$-RNT for 3, 6, or 12 hours showed a treatment-dependent effect on the total number of cells in bronchoalveolar lavage fluid. An increase in the number of polymorphonuclear cells in bronchoalveolar lavage fluid compared with saline controls was observed in mice treated with either LPS or K^{90}/$RGDSK^{10}$-RNT (Figure 3A). The administration of K^{90}/$RGDSK^{10}$–RNT and the LPS together caused significantly more recruitment of polymorphonuclear cells at 3, 6, and 12 hours compared with the animals treated with LPS only (Figure 3A). Mice challenged with LPS or K^{90}/$RGDSK^{10}$-RNT showed significantly more monocytes in bronchoalveolar lavage fluid compared with control mice, while mice administered both LPS and K^{90}/$RGDSK^{10}$-RNT had significantly more monocytes compared with all other groups at 6 hours (Figure 3B).

Protein levels in bronchoalveolar lavage fluid

LPS or K^{90}/$RGDSK^{10}$-RNT treatment significantly increased protein content in bronchoalveolar lavage fluid at 6 hours

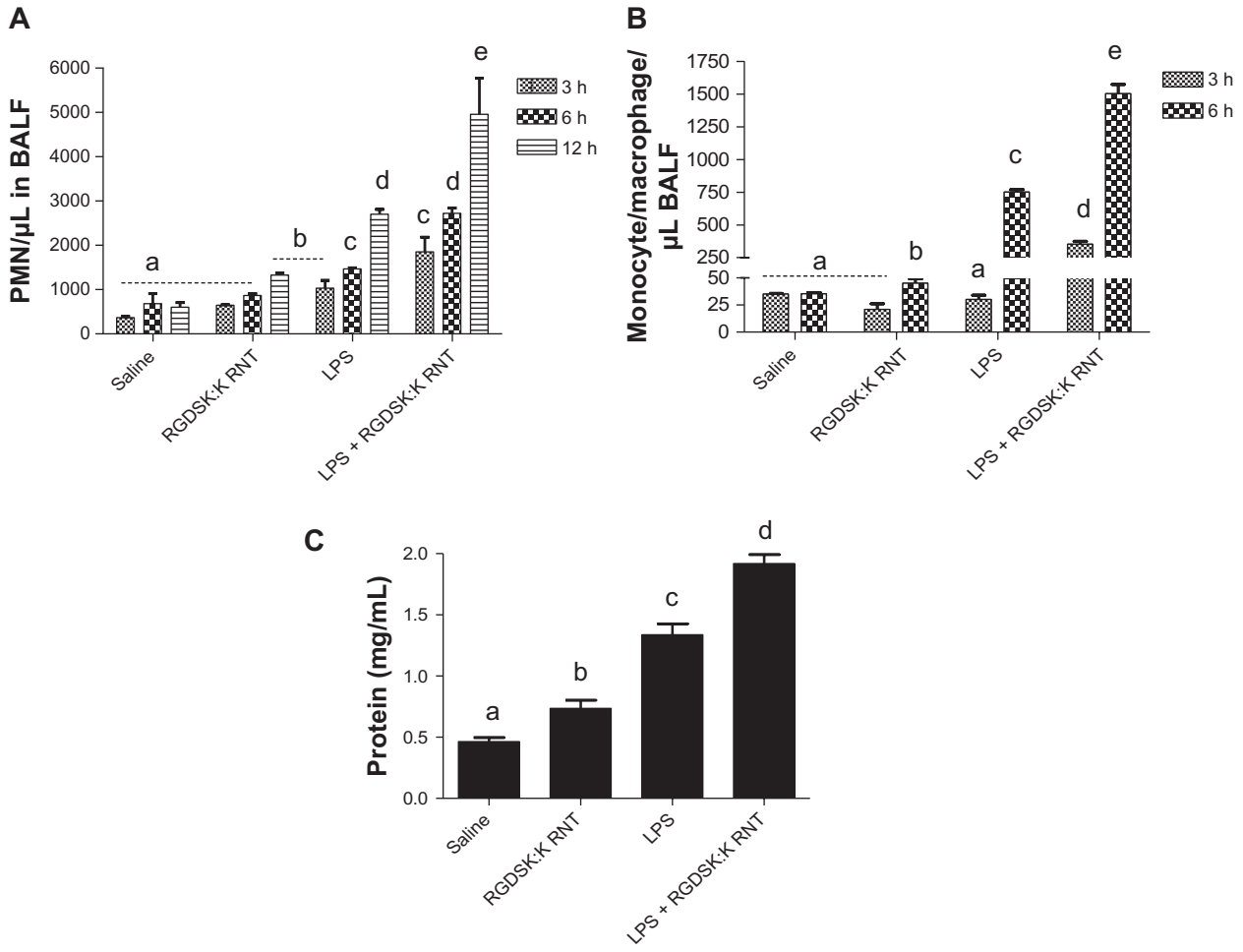

Figure 3 Differential cell count and protein in bronchoalveolar lavage fluid. Total and differential cell count was performed in bronchoalveolar lavage fluid 3, 6, or 12 hours following treatment. Numbers of polymorphonuclear cells in the bronchoalveolar lavage fluid were significantly higher in the lipopolysaccharide and K^{90}/$RGDSK^{10}$ rosette nanotube groups compared with saline controls. However, the lipopolysaccharide + K^{90}/$RGDSK^{10}$ rosette nanotube treatment group showed robust polymorphonuclear emigration at all time points (**A**). Lipopolysaccharide resulted in an increase in emigration of monocytes in bronchoalveolar lavage fluid after 6 hours (**B**). Treatment with K^{90}/$RGDSK^{10}$ rosette nanotubes had no effect on monocyte emigration compared with the saline control at all time points tested. Interestingly, mice treated with lipopolysaccharide and K^{90}/$RGDSK^{10}$ rosette nanotubes showed a significant increase in monocyte emigration. Total protein analysis in bronchoalveolar lavage fluid showed a significant increase in protein content in the lipopolysaccharide and K^{90}/$RGDSK^{10}$ rosette nanotube treatment groups (**C**). Interestingly, K^{90}/$RGDSK^{10}$ rosette nanotubes significantly proved the effect of lipopolysaccharide.

Note: Groups bearing different superscripts were significantly different ($P < 0.05$), while the groups with similar superscripts did not differ.

compared with the saline control (Figure 3C). Mice treated with LPS and K^{90}/RGDSK[10]-RNT showed significantly higher protein content in bronchoalveolar lavage fluid compared with the LPS group.

Myeloperoxidase in bronchoalveolar lavage fluid

The myeloperoxidase assay is used as a surrogate marker of neutrophil recruitment in inflamed lungs.[27] All treatment groups showed an increase in myeloperoxidase activity compared with the saline control (Figure 4). Mice treated with both K^{90}/RGDSK[10]-RNT and LPS showed significantly higher myeloperoxidase activity in bronchoalveolar lavage fluid compared with the LPS or RNT groups.

Interleukin-1β, MIP-1, MCP-1, and KC-1 expression in bronchoalveolar lavage

Interleukin-1β, MIP-1, MCP-1, and KC-1 are critical for the inflammatory response in the lungs. Mice treated with LPS or K^{90}/RGDSK[10]-RNT showed significantly increased concentrations of interleukin-1β, MIP-1, MCP-1, and KC-1 at the 3-hour and 6-hour time points compared with controls (Figure 5). The LPS + K^{90}/RGDSK[10]-RNT mice showed significantly more bronchoalveolar lavage fluid concentrations of these mediators compared with all other treatment groups. Expression of interleukin-1β and MCP-1 was higher at 6 hours compared with 3 hours in the mice given both LPS and K^{90}/RGDSK[10]-RNT (Figure 5). The RNT alone group had higher expression of the tested mediators compared with LPS only mice.

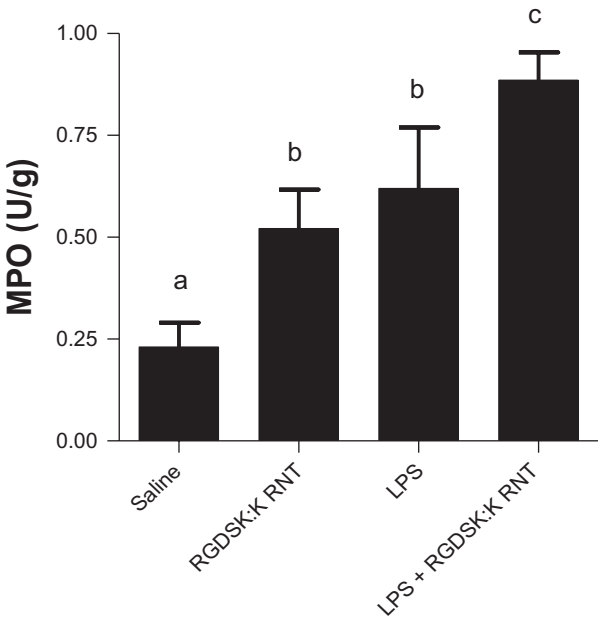

Figure 4 Myeloperoxidase assay in bronchoalveolar lavage fluid. A significant increase in myeloperoxidase was observed in all treatment groups compared with saline controls. Mice treated with K^{90}/RGDSK[10] rosette nanotubes and lipopolysaccharide showed significant higher myeloperoxidase activity in bronchoalveolar lavage fluid than the lipopolysaccharide group.

Interleukin-1β, MIP-1, MCP-1, and KC-1 mRNA expression in lung tissues

Mice treated with LPS or K^{90}/RGDSK[10]-RNT showed significantly higher expression of interleukin-1β, MIP-1, MCP-1, and KC-1 genes compared with the saline control, and that of interleukin-1β, and MCP-1 compared with LPS + K^{90}/RGDSK[10]-RNT mice. Expression of MIP-1 and KC-1 mRNA in the lungs of LPS + K^{90}/RGDSK[10]-RNT was more than the saline control (Figure 6).

Discussion

There is considerable effort underway to develop nanoparticles for therapeutic purposes. To achieve this goal, we need careful study of the biocompatibility of nanomaterials alone or in combination with other agonists, such as LPS in mammalian tissues.[3] We recently synthesized and characterized a biologically-inspired RNT that display RGD motif ligands for the integrin proteins on their surface, because integrins induce cell signals that regulate fundamental cell processes, such as cell migration, proliferation, and communication.[3,28] Therefore, we evaluated the very early lung effects of intravenously administered K^{90}/RGDSK[10]-RNT alone, or in combination with LPS in mice. The data show that K^{90}/RGDSK[10]-RNT alone induces very early lung inflammation and that RNT potentiates lung inflammation induced by LPS.

Acute lung inflammation is characterized by the migration of neutrophils and monocytes.[29] While neutrophils are the first cells to migrate into lungs challenged with LPS, monocytes exhibit a biphasic migration pattern.[30] The histological, myeloperoxidase, and bronchoalveolar lavage cell and protein data showed recruitment of neutrophils and monocytes into the lungs of mice challenged with LPS and thus validated the mouse model of LPS-induced lung inflammation used in these studies. Similar changes were induced in mice treated intravenously with K^{90}/RGDSK[10]-RNT alone. However, in sharp contrast with these results, earlier studies in C57BL/6 mice treated intranasally with lysine-functionalized RNT (assembled from twin G∧C bases) showed mild and transient lung inflammation.[13] In addition, an in vitro study showed that K-RNT (assembled form K-G∧C) neither reduces cell viability nor induces robust inflammation in human bronchial epithelial adenocarcinoma

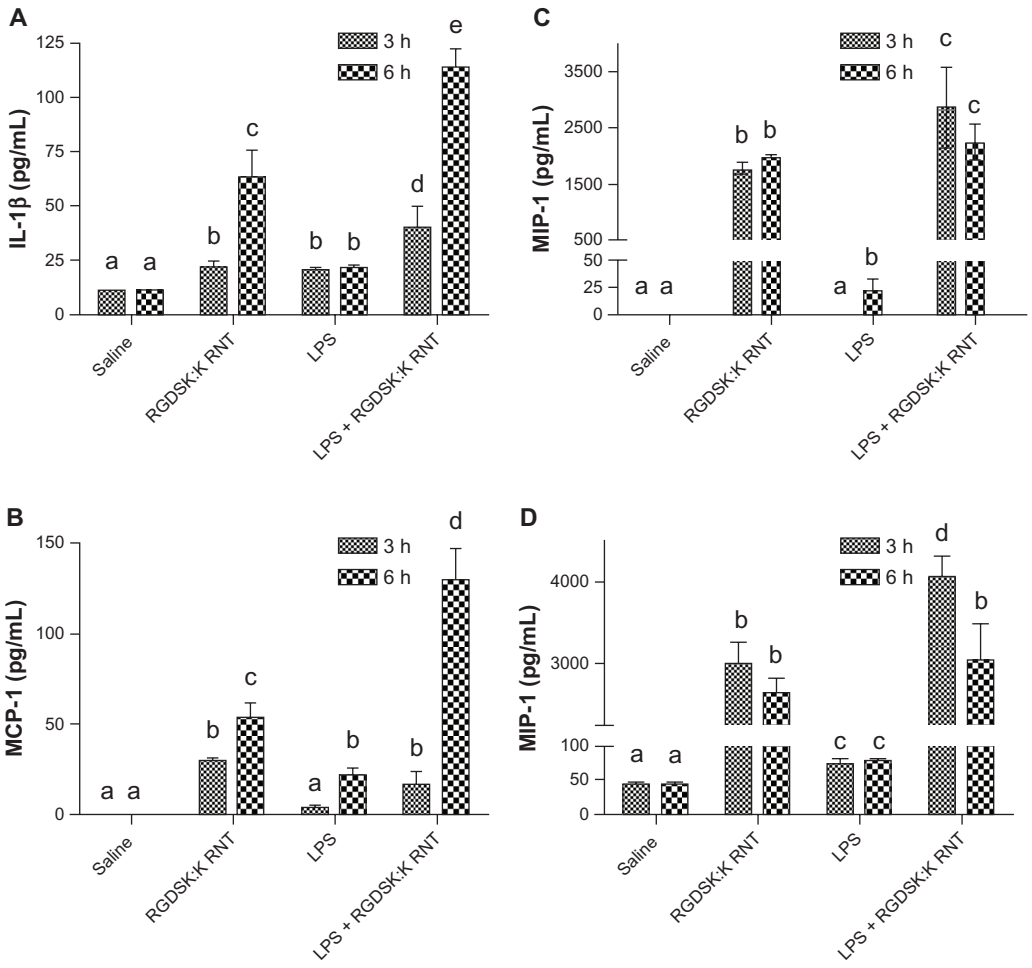

Figure 5 Secretion of proinflammatory cytokines. Lung homogenates from various treatment groups were analyzed for proinflammatory cytokines. Mice treated with K^{90}/$RGDSK^{10}$ rosette nanotubes showed a significant increase in secretion of interleukin-1β, MIP-1, MCP-1, and KC-1 compared with the saline control and lipopolysaccharide groups. Interestingly, the K^{90}/$RGDSK^{10}$ rosette nanotube + lipopolysaccharide group showed the highest levels of interleukin-1β, MIP-1, MCP-1, and KC-1.
Note: Groups bearing different superscripts were significantly different ($P < 0.05$), while the groups with similar superscripts did not differ.
Abbreviations: IL-1beta, interleukin-1beta; MCP-1, monocyte chemoattractant protein-1; KC-1, keratinocyte-dereived chemokine-1; MIP-1, macrophage inflammatory protein-1; ICAM, intercellular adhesion molecule.

Calu-3 cells and macrophages.[12,14] Because we examined only the 24-hour time point in the previous studies, it is possible that we may have missed acute lung inflammation at early time points, such as 6 hours. Another likely possibility is that RNTs that do not display the RGD peptide sequence may not activate the integrin-based signaling pathways. Activation of αvβ3 integrin signaling can result in increased endothelial permeability and potential migration of neutrophils.[31] We have previously shown expression of integrin αvβ3 on lung epithelium and endothelium,[22] which may have provided a receptor for RGD-RNT and resulted in inflammatory outcomes compared with nanotubes administrated intratracheally. We have recently reported that RGD-conjugated RNTs do activate cell signals, including P38 mitogen-activated protein kinase, leading to production of cytokines such as tumor necrosis factor-α in vitro, and similar pathways are also activated following binding of the integrin αvβ3.[16] Although we expect that lung inflammation induced by K^{90}/$RGDSK^{10}$-RNT may be transient, there is a need for further studies to clarify this theory.

The more intriguing aspect of the present work, however, is the apparent potentiation of the inflammatory effects of LPS by K^{90}/$RGDSK^{10}$-RNT. Recruitment of inflammatory cells occurs through early expression of cytokines, such as interleukin-1β, that induce activation of vascular endothelium and expression of adhesion molecules that cause induction of adhesion molecule expression. In LPS-induced lung inflammation, interleukin-1β is expressed very early in inflammation.[32] We found that while the protein concentrations of interleukin-1β were higher in bronchoalveolar lavage fluid from both LPS or K^{90}/$RGDSK^{10}$-RNT mice, expression was significantly enhanced in mice

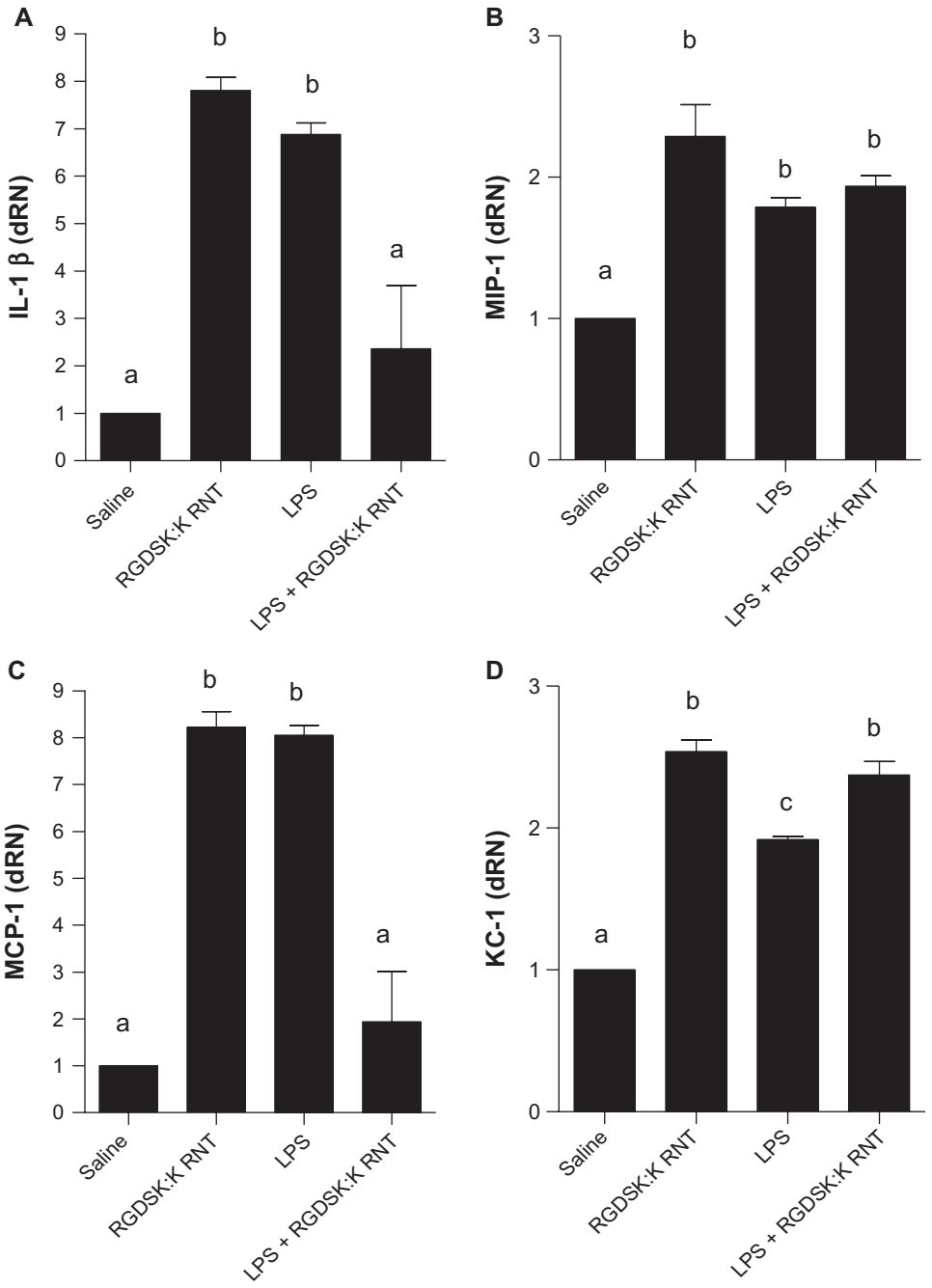

Figure 6 Expression of proinflammatory cytokines. The lipopolysaccharide and K^{90}/RGDSK[10] rosette nanotube groups showed significantly higher expression of proinflammatory genes compared with saline controls. Mice treated with K^{90}/RGDSK[10] rosette nanotubes following lipopolysaccharide challenge showed significant inhibition of interleukin-1β and MIP-1, and an increase in KC-1 mRNA transcripts when compared with the lipopolysaccharide group. MIP-1 expression did not differ between the lipopolysaccharide and lipopolysaccharide + K^{90}/RGDSK[10] rosette nanotube groups.

Note: Groups bearing different superscripts were significantly different ($P < 0.05$), while the groups with similar superscripts did not differ.

treated with both agonists. A similar pattern was observed for mRNA expression of interleukin-1β in lung tissues from mice given various treatments. Migration of neutrophils and monocytes is a complex process and is induced by the expression of chemokines such as MIP-1, KC-1, and MCP-1.[33] Protein expression of MIP-1 and KC-1, which are central to migration of neutrophils, and MCP-1, which is critical for recruitment of monocytes, was found to be significantly higher in the bronchoalveolar lavage fluid of mice treated with a combination of LPS and K^{95}/RGDSK[5]-RNT compared with those treated with LPS or K^{90}/RGDSK[10]-RNT alone, as well as saline alone. An important observation is that levels of interleukin-1β and MCP-1 were significantly higher at 6 hours compared with 3 hours in mice exposed

to both LPS and K^{90}/RGDSK^{10}-RNT compared with the other groups. This increase at 6 hours would be critical in sustaining the migration of neutrophils and monocytes at later time points that we did not pursue. However, it is well established that, contrary to the prevailing belief, monocytes can also migrate into the lung as early as 6 hours following LPS treatment, followed by another increase at 24 hours.[30] On the other hand, neutrophils, which are important for the migration of monocytes into inflamed lungs, showed a sustained increase up to 24 hours followed by a decline.[30] Our previous observation of mild inflammation 24 hours after intratracheal administration of K-RNT alone suggests that dual treatments with LPS and K^{90}/RGDSK^{10}-RNT may result in a more aggravated inflammatory response in the lungs. Although the expression of inflammatory mediators does suggest a mechanistic framework, there is a need for experiments using β3-deficient mice to elucidate the role of αvβ3 integrin in lung inflammation induced by treatment with K^{90}/RGDSK^{10}-RNT.

It is evident from the literature that, in acute lung inflammation, activated endothelial cells produce intercellular adhesion molecule-1 that contains a RGD motif, which is known to interact with leukocyte integrin αvβ3, resulting in anchoring of neutrophils to endothelial cells (Figure 7A). Therefore, targeting neutrophil integrin αvβ3 with its ligand, RGDSK (peptide or RNT), might block free available integrin αvβ3 receptors that may inhibit its transmigration across endothelial cells (Figure 7B). This suggestion was recently

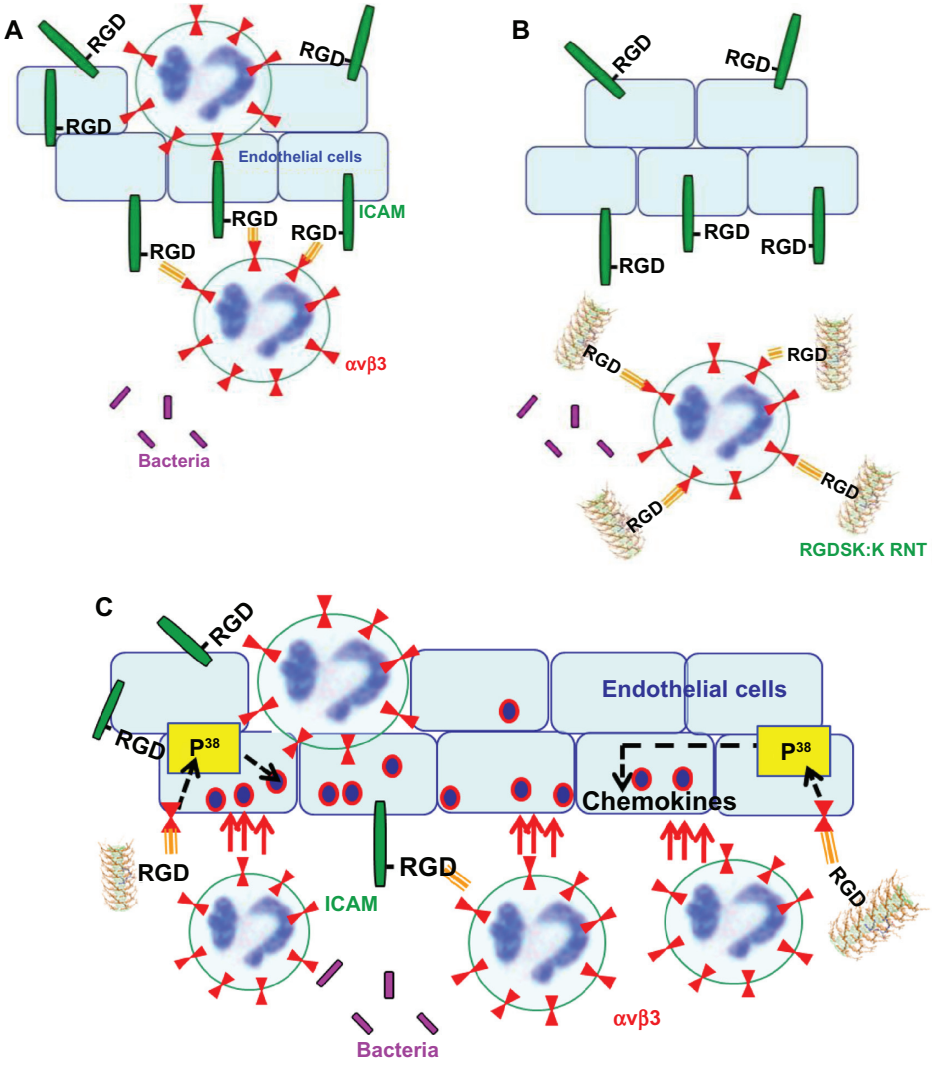

Figure 7 Possible mechanism of action of RGDSK:K rosette nanotubes in vivo. In acute lung inflammation, activated endothelial cells produce intercellular adhesion molecule-1 that contains a RGD motif, which is known to interact with leukocyte integrin αvβ3 resulting in the attachment of leukocytes to endothelial cells (**A**). Therefore, targeting neutrophil integrin αvβ3 with RGDSK (peptide or rosette nanotubes) might block free available receptors that may inhibit its transmigration across endothelial cells (**B**). Here we propose that K^{90}/RGDSK^{10} rosette nanotubes might be the triggering P38 mitogen-activated protein kinase cascade in vivo that upregulates the proinflammatory response (**C**).

supported by Moon et al who demonstrated inhibition of neutrophil transmigration by RGDS synthetic peptide.[34] However, RNTs and cyclic peptides are not comparable due to differences in their physical and chemical dimensions, which might have contributed to the different trend in our mouse model. We previously reported a P38 mitogen-activated protein kinase-dependent proinflammatory response of K^{90}/$RGDSK^{10}$-RNT while the role of P38 mitogen-activated protein kinase in transmigration of neutrophils and lung inflammation is well documented.[16,34–36] Based on these reports we propose that K^{90}/$RGDSK^{10}$-RNT might trigger a P38 mitogen-activated protein kinase cascade in vivo that upregulates the proinflammatory response (Figure 7C).

Conclusion

While our previous in vivo study demonstrated the noninflammatory nature of K-RNT,[14] its seemingly minor alteration by co-assembly with an RGDSK–RNT to form a hybrid nanotube (ie, K^{90}/$RGDSK^{10}$-RNT) did promote strong lung inflammation. In addition, K^{90}/$RGDSK^{10}$-RNT administered intravenously immediately after intranasal LPS treatment was found to aggravate the immune response significantly. Based on these results and earlier reports,[16, 34-36] we postulate that K^{90}/$RGDSK^{10}$-RNT induces a P38 MAP kinase cascade in vivo that upregulates the proinflammatory response.

Acknowledgments

We thank the National Research Council, The University of Alberta, the Natural Science and Engineering Research Council, the Canada Foundation for Innovation, and Alberta Agriculture Research Institute for supporting this research program.

Disclosure

The authors report no conflicts of interest in this work.

References

1. Nel A, Xia T, Madler L, Li N. Toxic potential of materials at the nanolevel. *Science*. 2006;311(5761):622–627.
2. Roco MC. Science and technology integration for increased human potential and societal outcomes. *Ann N Y Acad Sci*. 2004;1013:1–16.
3. Suri SS, Fenniri H, Singh B. Nanotechnology-based drug delivery systems. *J Occup Med Toxicol*. 2007;2:16.
4. Oyelere AK, Chen PC, Huang X, El-Sayed IH, El-Sayed MA. Peptide-conjugated gold nanorods for nuclear targeting. *Bioconjug Chem*. 2007;18(5):1490–1497.
5. Tkachenko AG, Xie H, Liu Y, et al. Cellular trajectories of peptide-modified gold particle complexes: comparison of nuclear localization signals and peptide transduction domains. *Bioconjug Chem*. 2004; 15(3):482–490.
6. Fenniri H, Deng BL, Ribbe AE. Helical rosette nanotubes with tunable chiroptical properties. *J Am Chem Soc*. 2002;124(37):11064–11072.
7. Fenniri H, Deng BL, Ribbe AE, Hallenga K, Jacob J, Thiyagarajan P. Entropically driven self-assembly of multichannel rosette nanotubes. *Proc Natl Acad Sci U S A*. 2002;99 Suppl 2:6487–6492.
8. Fenniri H, Mathivanan P, Vidale KL, et al. Helical rosette nanotubes: design, self-assembly, and characterization. *J Am Chem Soc*. 2001; 123(16):3854–3855.
9. Johnson RS, Yamazaki T, Kovalenko A, Fenniri H. Molecular basis for water-promoted supramolecular chirality inversion in helical rosette nanotubes. *J Am Chem Soc*. 2007;129(17):5735–5743.
10. Moralez JG, Raez J, Yamazaki T, Motkuri RK, Kovalenko A, Fenniri H. Helical rosette nanotubes with tunable stability and hierarchy. *J Am Chem Soc*. 2005;127(23):8307–8309.
11. Raez J, Moralez JG, Fenniri H. Long-range flow-induced alignment of self-assembled rosette nanotubes on Si/SiOx and poly(methyl methacrylate)-coated Si/SiOx. *J Am Chem Soc*. 2004;126(50):16298–16299.
12. Journeay WS, Suri SS, Moralez JG, Fenniri H, Singh B. Macrophage inflammatory response to self-assembling rosette nanotubes. *Small*. 2009;5(12):1446–1452.
13. Journeay WS, Suri SS, Moralez JG, Fenniri H, Singh B. Rosette nanotubes show low acute pulmonary toxicity in vivo. *Int J Nanomedicine*. 2008;3(3):373–383.
14. Journeay WS, Suri SS, Moralez JG, Fenniri H, Singh B. Low inflammatory activation by self-assembling Rosette nanotubes in human Calu-3 pulmonary epithelial cells. *Small*. 2008;4(6):817–823.
15. Humphries JD, Byron A, Humphries MJ. Integrin ligands at a glance. *J Cell Sci*. 2006;119(Pt 19):3901–3903.
16. Suri SS, Rakotondradany F, Myles AJ, Fenniri H, Singh B. The role of RGD-tagged helical rosette nanotubes in the induction of inflammation and apoptosis in human lung adenocarcinoma cells through the P38 MAPK pathway. *Biomaterials*. 2009;30(17):3084–3090.
17. Matthay MA. Treatment of acute lung injury: clinical and experimental studies. *Proc Am Thorac Soc*. 2008;5(3):297–299.
18. Zemans RL, Colgan SP, Downey GP. Transepithelial migration of neutrophils: mechanisms and implications for acute lung injury. *Am J Respir Cell Mol Biol*. 2009;40(5):519–535.
19. Mizgerd JP. Molecular mechanisms of neutrophil recruitment elicited by bacteria in the lungs. *Semin Immunol*. 2002;14(2):123–132.
20. Gonzalez AL, El-Bjeirami W, West JL, McIntire LV, Smith CW. Transendothelial migration enhances integrin-dependent human neutrophil chemokinesis. *J Leukoc Biol*. 2007;81(3):686–695.
21. Lawson MA, Maxfield FR. Ca2+- and calcineurin-dependent recycling of an integrin to the front of migrating neutrophils. *Nature*. 1995;377: 75–79.
22. Singh B, Fu C, Bhattacharya J. Vascular expression of the alpha(v) beta(3)-integrin in lung and other organs. *Am J Physiol*. 2000;278: L217–L226.
23. Borzsonyi G, Johnson RS, Myles AJ, et al. Rosette nanotubes with 1.4 nm inner diameter from a tricyclic variant of the Lehn-Mascal G – C base. *Chem Commun (Camb)*. 2010;46(35):6527–6529.
24. Tikhomirov G, Yamazaki T, Kovalenko A, Fenniri H. Hierarchical self-assembly of organic prolate nanospheroids from hydrophobic rosette nanotubes. *Langmuir*. 2008;24(9):4447–4450.
25. Charavaryamath C, Juneau V, Suri SS, Janardhan KS, Townsend H, Singh B. Role of Toll-like receptor 4 in lung inflammation following exposure to swine barn air. *Exp Lung Res*. 2008;34(1):19–35.
26. Schneider T, Issekutz AC. Quantitation of eosinophil and neutrophil infiltration into rat lung by specific assays for eosinophil peroxidase and myeloperoxidase. Application in a Brown Norway rat model of allergic pulmonary inflammation. *J Immunol Methods*. 1996;198(1):1–14.
27. Faith M, Sukumaran A, Pulimood AB, Jacob M. How reliable an indicator of inflammation is myeloperoxidase activity? *Clin Chim Acta*. 2008;396(1–2):23–25.
28. Kobayashi-Sakamoto M, Isogai E, Hirose K, Chiba I. Role of alpha v integrin in osteoprotegerin-induced endothelial cell migration and proliferation. *Microvasc Res*. 2008;76(3):139–144.
29. Martin TR, Nakamura M, Matute-Bello G. The role of apoptosis in acute lung injury. *Crit Care Med*. 2003;31(4 Suppl):S184–S188.

30. Janardhan KS, Sandhu SK, Singh B. Neutrophil depletion inhibits early and late monocyte/macrophage increase in lung inflammation. *Front Biosci*. 2006;11:1569–1576.
31. Tsukada H, Ying X, Fu C, et al. Ligation of endothelial alpha v beta 3 integrin increases capillary hydraulic conductivity of rat lung. *Circ Res*. 1995;77:651–659.
32. Ingram JL, Rice AB, Geisenhoffer K, Madtes DK, Bonner JC. IL-13 and IL-1beta promote lung fibroblast growth through coordinated up-regulation of PDGF-AA and PDGF-Ralpha. *FASEB J*. 2004;18(10):1132–1134.
33. Puneet P, Moochhala S, Bhatia M. Chemokines in acute respiratory distress syndrome. *Am J Physiol Lung Cell Mol Physiol*. 2005;288(1): L3–L15.
34. Moon C, Han JR, Park HJ, Hah JS, Kang JL. Synthetic RGDS peptide attenuates lipopolysaccharide-induced pulmonary inflammation by inhibiting integrin signaled MAP kinase pathways. *Respir Res*. 2009; 10:18.
35. Nick JA, Young SK, Arndt PG, et al. Selective suppression of neutrophil accumulation in ongoing pulmonary inflammation by systemic inhibition of p38 mitogen-activated protein kinase. *J Immunol*. 2002;169(9):5260–5269.
36. Koshio O, Tansho S, Ubagai T, Nakaki T, Ono Y. Suppression of phosphorylation of extracellular-signal-regulated kinase and p38 mitogen-activated protein kinase in polymorphonuclear leukocytes by the proton pump inhibitor lansoprazole. *J Infect Chemother*. 2010; 16(2):100–106.